

phys. stat. sol. (a) **59**, 673 (1980)

Subject classification: 18.2; 21.1

Institute of Solid State Physics, Academy of Sciences of the USSR, Chernogolovka¹⁾

The Magnetic Properties of Ni-Mn-H Solid Solutions

By

V. E. ANTONOV, I. T. BELASH, and V. G. THIESEN

The behaviour of the Curie points at $P_{H_2} \lesssim 15$ kbar and of the magnetization at atmospheric pressure and $4.2 \leq T \lesssim 100$ K is investigated for hydrogen solid solutions on the base of disordered f.c.c. Ni-Mn alloys containing 10, 20, and 30 at% Mn. The samples for the magnetization measurements are hydrogenated at $P_{H_2} \leq 70$ kbar. It is shown that the observed effects may be explained within the framework of the band theory of magnetism considering hydrogen as a donor of a fractional quantity of electrons.

У растворов водорода на базе неупорядоченных ГЦК сплавов Ni-Mn, содержащих 10, 20 и 30 ат% Mn, исследовано поведение точек Кюри при $P_{H_2} \lesssim 15$ кбар и намагниченности при атмосферном давлении и $4,2 \leq T \lesssim 100$ К. Образцы для измерения намагниченности насыщали водородом при $P_{H_2} \leq 70$ кбар. Показано, что наблюдаемые эффекты могут быть объяснены в рамках зонной теории магнетизма, если считать водород донором дробного числа электронов.

1. Introduction

The effect of hydrogen on the magnetic properties of the Ni-Fe [1], $Fe_{65}(Ni_{1-x}Mn_x)_{35}$ [2], and Ni-Co [3] γ -alloys (with f.c.c. crystal lattice of the metal) turned out to be similar to that on changing the composition of the starting samples towards the enriching with the elements having a greater number of $3d + 4s$ electrons. Since the dependence of the properties of most of these alloys (at least of Ni-Co and Ni-Fe non-invar alloys) upon composition is determined mainly by the electron concentration [4], the results of [1 to 3] allowed a qualitative description of the magnetic properties of the mentioned Me-H solid solutions with hydrogen considered as a donor of a fractional quantity of electrons [2, 3].

As has been noted in [3], the calculations of the band structures of γ -hydrides of some transition metals [5 to 8] may serve as a basis for such a description. These calculations indicate that although the rigid band model cannot be used to describe the Me-H solid solutions, the changes of the states of d-symmetry of the host metals under hydrogenation are considerably weaker than those of sp-states. At the atomic ratio H-to-metal $n \leq 1$, no new (hydrogen) electronic band is formed below the Fermi energy, an increase of hydrogen content in the metal resulting in an increase of the degree of occupation of d-states, while it is the d-band structure and the degree of its occupation that mainly determine the magnetic properties of transition metals.

The available experimental evidence makes it possible now to consider the more involved case of hydrogen solid solutions in Ni-Cr and Ni-Mn alloys, where the composition dependence of the magnetic properties is strongly affected by the changes of the band structure [4]. Hydrogenation of the Ni-Cr γ -alloys containing ≤ 7 at% Cr has been shown to lower the Curie points T_C and the spontaneous magnetization σ_0 at $T = 0$ K [9]. The Ni-Mn-H solutions have been studied in [10, 11] at temperatures close to room temperature. The present work is devoted to the investigation of the behaviour of T_C and σ_0 of Ni-Mn-H solid solutions based on the disordered f.c.c. Ni-Mn alloys containing 10, 20, and 30 at% Mn. On the grounds of the data of [1 to

¹⁾ Chernogolovka 142 432, Moscow district, USSR.

3, 9] and the present work, a description of the dependence of magnetic properties of Me-H γ -solutions based on transition metals and their alloys upon hydrogen concentration has been proposed within the framework of the band theory of ferromagnetism.

2. Experimental

The ingots were melted in an induction furnace under an argon atmosphere from electrolytical nickel and manganese. After a 6 h homogenization at 1400 K and water quenching, these ingots were rolled into thick sheets ≈ 0.5 mm. Then the sheets were subjected to stress-relief annealing at 1400 K for 3 min, quenched in water to obtain the disordered state at normal conditions [12], and chemically etched to the thickness of ≈ 0.2 mm. The samples were prepared from this foil.

Alloying of nickel with manganese lowers the kinetic stability of Me-H solid solutions in regard to the desintegration into metal and molecular hydrogen [10]. In our case, the solutions on the base of the alloy with 30 at% Mn began to lose hydrogen with noticeable rate at temperatures beyond ≈ 170 to 220 K (at room temperature the samples completely decompose in about 3 min). Hydrogenation of the samples was conducted by several hours exposure under hydrogen pressures up to 70 kbar and $T = 520$ K with subsequent quenching down to 150 K [3].

The magnetization was measured with an accuracy of 8% at normal pressure in a pulsed magnetic field $H \leq 45$ kOe by the induction method [13] in the temperature range 4.2 to 100 K, the pulse duration being ≈ 0.01 s. The Curie points of the alloys under high pressure were determined by the differential transformer method [14, 3] by controlling the position of the anomalies of the temperature dependence curve of the initial magnetic permeability $\mu_0(T)$ with an accuracy of ± 3 K in an inert medium (silicon) and ± 5 K in hydrogen. At pressures up to 20 kbar the experimental errors did not exceed ± 1 and ± 3 K in temperature and ± 0.2 and ± 0.5 kbar in pressure, in an inert medium and in hydrogen, respectively. Then the measurements were performed in hydrogen, the thermocouple (chromel-alumel) and the manganin wire gauge were protected from direct exposure to hydrogen.

The hydrogen content in the Me-H samples was measured with 5% error by collecting the released hydrogen to a scaled glass vessel (silicon being expelled from the vessel) at atmospheric pressure and room temperature.

3. Results

3.1 Phase T - P_{H_2} diagram of the Ni-Mn-H system

In nickel under high hydrogen pressure the isomorphic transition $\gamma_1 \rightleftharpoons \gamma_2$ [15] occurs whose line in the T - P_{H_2} diagram terminates in a critical point with the coordinates $620 < T_{cr} < 700$ K, $16 < (P_{H_2})_{cr} < 19$ kbar [16, 17]. Alloying of nickel with manganese results in lowering T_{cr} to room temperature at ≈ 18 at% of Mn [18], solubility of hydrogen at $T \geq 298$ K thus becoming a continuous function of pressure in alloys with a greater manganese content.

Fig. 1 shows the electric resistance isotherms for the alloy with 10 at% Mn at a step-wise increase and decrease of hydrogen pressure. At every point presented in Fig. 1 the sample was exposed for a time $\Delta\tau$ up to the termination of the resistance drift $R(\tau)$ caused by the diffusional nature of the formation of Ni-Mn-H solid solutions, and the final value of R was plotted in the figure. The characteristic values of $\Delta\tau$ were of the same order of magnitude as in the Ni-Fe-H system [16]. It is seen from Fig. 1 that at 423 K there are well localized resistance jumps of the $R(P_{H_2})$ isotherms corresponding to the $\gamma_1 \rightarrow \gamma_2$ and $\gamma_2 \rightarrow \gamma_1$ phase transitions. The transformation possesses a noticeable hysteresis (≈ 1 kbar) that points to its first-order nature at

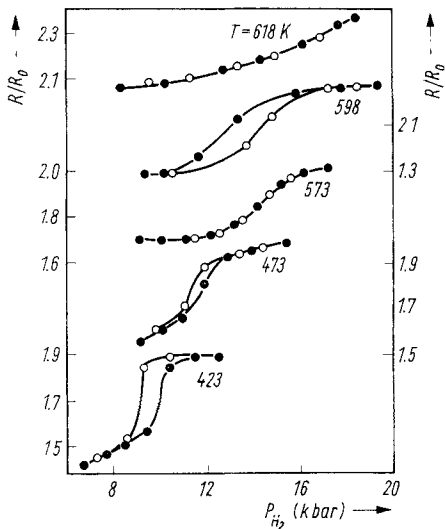


Fig. 1

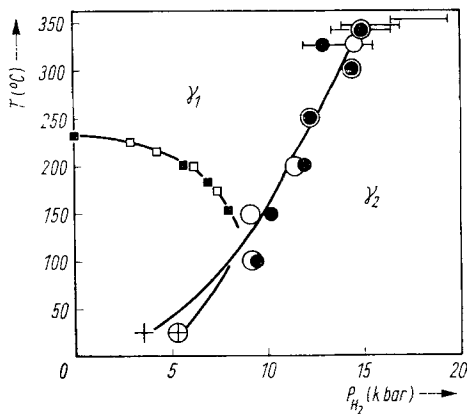


Fig. 2

Fig. 1. Electrical resistance isotherms of the $\text{Ni}_{90}\text{Mn}_{10}$ alloy in hydrogen atmosphere. ● — increasing pressure, ○ — decreasing pressure. R_0 is the resistance of the sample at normal conditions

Fig. 2. T - P_{H_2} phase diagram of the $\text{Ni}_{90}\text{Mn}_{10}$ -H system. ● pressures of the $\gamma_1 \rightarrow \gamma_2$ transition, ○ $\gamma_2 \rightarrow \gamma_1$, — regions of the supercritical anomalies of electrical resistance, ■, □ Curie points at a step-wise increase and decrease of pressure, respectively

this temperature. At 563 K the hysteresis disappears, and the resistance anomaly becomes more sloping. Further increase of temperature results in a decrease of the amplitude of this anomaly. This kind of behaviour is typical for supercritical resistance isotherms [16]. A rough estimate yields $T_{\text{cr}} = (600 \pm 30)$ K. The positions of the anomalies of the isotherms $R(P_{\text{H}_2})$ are plotted in the T - P_{H_2} phase diagram Fig. 2. The obtained curves of $\gamma_1 \rightarrow \gamma_2$ and $\gamma_2 \rightarrow \gamma_1$ transformations for the $\text{Ni}_{90}\text{Mn}_{10}$ -H system do not differ strongly from those for the Ni-H system [17].

Note that the $T_{\text{cr}}(x_{\text{Mn}})$ dependence for the studied system is considerably non-linear: the rate of T_{cr} decreasing grows with the increase of the atomic fraction x_{Mn} in Ni-Mn alloys. For instance, a 10 at% Mn addition to nickel results in a decrease of the critical temperature by $T_{\text{cr}}(0) - T_{\text{cr}}(0.1) \approx T_{\text{cr}}^{\text{Ni}} - 600 \lesssim 100$ K, while a further 8 at% Mn addition results in $T_{\text{cr}}(0.1) - T_{\text{cr}}(0.18) \approx 300$ K. The $T_{\text{cr}}(x_{\text{Fe}})$ dependence for the Ni-Fe-H system has a similar character [16, 19].

3.2 The Curie points and spontaneous magnetization of Ni-Mn-H solid solutions

The $\sigma_0(x_{\text{Mn}})$ dependence for the disordered f.c.c. Ni-Mn alloys is non-monotonic. For pure nickel $\sigma_0(0) \approx 0.606 \mu_{\text{B}}/\text{atom}$; as manganese is substituted for nickel σ_0 grows, reaches the maximum value $\sigma_0(0.1) \approx 0.8 \mu_{\text{B}}/\text{atom}$ for $x_{\text{Mn}} \approx 0.1$, subsequently beginning to decrease [20].

The Curie points steadily decrease from 630 K for nickel to helium temperatures at $x_{\text{Mn}} \approx 0.26$. The measurements carried out in the present work at $P \leq 15$ kbar have shown that in an inert medium the Curie points of the Ni-Mn alloys with 10 and 20 at% Mn approximately linearly decrease with pressure (the dT_{C}/dP)_{in} values

Table 1

x_{Mn}	T_C (K)	$\sigma_0(\mu_B/\text{atom})$	$(dT_C/dP)_{in}$ (K kbar $^{-1}$)	ξ	ζ
0.1	506	0.80	-0.65 ± 0.2	—	—
0.2	353	0.62	-0.30 ± 0.1	0.27	0.81
0.3	—	0	—	0.16	0.48

$$\xi = -\Delta x_{Mn}/\Delta n, \zeta = \Delta N^e/\Delta n = 3\xi$$

are shown in Table 1. At a high hydrogen pressure, due to the diffusional nature of the formation of Ni-Mn-H solid solution, time dependences $T_C(\tau)$ appeared at a fixed P_{H_2} after a change of pressure. As well as in the case of resistance measuring, the samples were exposed at each selected P_{H_2} up to the termination of the time drift $T_C(\tau)$ and the final T_C value was plotted in the diagram. The obtained $T_C(P_{H_2})$ dependences for the alloys with 10 and 20 at% Mn are shown in Fig. 2 and 3, respectively. The $\sigma_0(n)$ dependences for the studied γ -solutions Ni-Mn-H are shown in Fig. 4. As in [2, 3], the σ_0 and T_C values of Me-H specimens metastable at atmospheric pressure were obtained using the equations of the theory of very weak itinerant ferromagnetism [21].

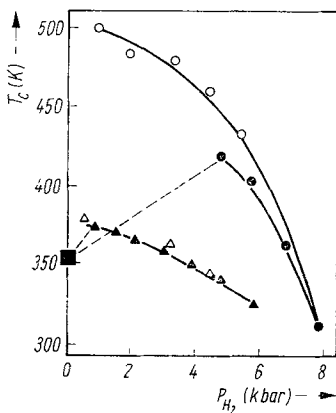


Fig. 3

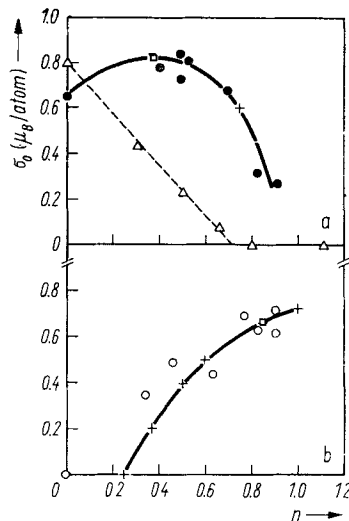


Fig. 4

Fig. 3. Curie point dependence on hydrogen pressure for the Ni₈₀Mn₂₀ alloy. ■ T_C of the starting samples; ▲, △ data obtained at increasing and lowering pressure, respectively, after initial saturation of the sample with hydrogen at $T = 420$ K and $P_{H_2} = 0.8$ kbar; ●, ○ the same for the sample initially saturated with hydrogen at $T = 420$ K and $P_{H_2} = 4.8$ kbar

Fig. 4. Spontaneous magnetization σ_0 at $T = 0$ K in dependence on hydrogen content n in the Ni-Mn alloys with △ 10, ● 20, ○ 30 at% Mn; □ σ_0 values used to calculate ξ and ζ ; × calculated values of $\sigma_0(n)$, see the text. The magnetization is given in μ_B/atom of the Ni-Mn alloy

3.2.1 $Ni_{90}Mn_{10}$ -H solutions

As is seen from Fig. 2, T_C of the γ_1 phase of this system steadily decreases with hydrogen pressure until the intersection of the Curie point line with the $\gamma_1 \rightarrow \gamma_2$ transition curve at $P_{H_2} \approx 9$ kbar, $\Delta T_C = T_C(P_{H_2} = 9 \text{ kbar}) - T_C(P = 1 \text{ bar})$ being ≈ -100 K. In an inert medium a pressure of 9 kbar results in lowering the Curie point of the $Ni_{90}Mn_{10}$ alloy by $\approx |(dT_C/dP)|_{in} 9 = (6 \pm 2)$ K (see Table 1). Consequently, the considerable decrease of T_C observed in hydrogen atmosphere is caused by an increase of the hydrogen solubility in the γ_1 -phase of the $Ni_{90}Mn_{10}$ -H system with increasing pressure. Measurement under high hydrogen pressure indicated that the γ_2 -phase of this system is paramagnetic at $T \geq 300$ K and $P_{H_2} \leq 20$ kbar.

The hydrogen mobility in Ni-H solutions was shown to be so large that even at $T < 250$ K the separation into the γ_1 and γ_2 phases occurs in accordance with the equilibrium T - C diagram, the compositions of the phases coexisting at $P = 1$ atm being $n_{\gamma_1}^{max} < 0.02$ and $n_{\gamma_2}^{min} = 0.7 \pm 0.05$ [22]. A similar separation should be observed in solutions based on the $Ni_{90}Mn_{10}$ alloy due to their high T_{cr} value. Since the temperature of our Ni-Mn-H specimens at $P = 1$ atm never exceeded 150 K (see Section 2), the observed values of $n_{\gamma_1}^{max}$ and $n_{\gamma_2}^{min}$ are the equilibrium ones for $T \lesssim 150$ K, if of course, the kinetics of the separation allows to approach equilibrium at these temperatures (note that the $n_{\gamma_1}^{max}$ and $n_{\gamma_2}^{min}$ values at normal pressure may differ strongly from those at high hydrogen pressure; so, in the Ni-H system, as mentioned above, $n_{\gamma_2}^{min} \approx 0.7$ at $P = 1$ atm and $T < 250$ K whereas $n_{\gamma_2}^{min} \approx 1$ under nearly equilibrium hydrogen pressure at room temperature [17, 23]). As will be shown later, in the $Ni_{90}Mn_{10}$ -H system the hydrogen mobility seems to be large enough to ensure an equilibrium phase composition of the samples at $P = 1$ atm and $T \lesssim 150$ K.

An X-ray study ($P = 1$ atm, $T = 77$ K) has shown the $Ni_{90}Mn_{10}$ -H specimens with $n \geq 0.75$ to be single-phase [18], i.e. $n_{\gamma_2}^{min} \lesssim 0.75$. According to the similar study at $P = 1$ atm and $T = 83$ K, the specimens with $n \leq 0.5$ consist of two phases: pure metal and hydride. Since hydrogenation leads to an increase of the unit cell volume V_0 of the Ni-Mn f.c.c. sublattice with the slope $\beta = (\partial/\partial n) V_0 \approx 10 \text{ \AA}^3$ [18], and the accuracy of the X-ray measurement was $\delta V_0 \lesssim 0.3 \text{ \AA}^3$, the observed absence of volume expansion due to the presence of hydrogen in the γ_1 phase of the two-phase specimens with $n \leq 0.5$ gives $n_{\gamma_1}^{max} \leq \delta V_0/\beta \lesssim 0.03$.

The $\sigma_0(n)$ dependence at atmospheric pressure for the alloy with 10 at% Mn is shown in Fig. 4a. At $n \leq 0.66$ (or in the region of hydrogen contents where the sample should consist of a mixture of the γ_1 and γ_2 phases) σ_0 approximately linearly decreases as hydrogen concentration increases. The $Ni_{90}Mn_{10}$ -H solutions with $n \geq 0.8$ do not possess a spontaneous magnetization in the range of temperatures studied.

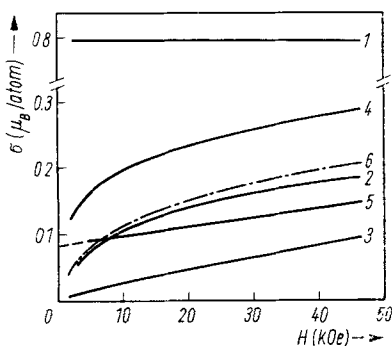


Fig. 5. Magnetization isotherms $\sigma(H)$ for some of the $Ni_{90}Mn_{10}$ -H solid solutions. (1) $n = 0$, $T = 4.2$ K; (2, 3) $n = 1.11$, $T = 4.2$ and 73 K; (4, 5) $n = 0.66$, $T = 4.2$ and 100 K; (6) $(\sigma_{4.2}^{0.66}(H))_{\gamma_2}$ dependence, see the text

The $\sigma(H)$ dependences for some of the $\text{Ni}_{90}\text{Mn}_{10}\text{-H}$ samples are shown in Fig. 5. It is seen (curve 1) that the magnetization of the $\text{Ni}_{90}\text{Mn}_{10}$ alloy at $H \leq 45$ kOe does not depend upon the magnetic field within the experimental error. Within this error the temperature dependence of the magnetization of the $\text{Ni}_{90}\text{Mn}_{10}$ sample is absent, too. The magnetization of the $\text{Ni}_{90}\text{Mn}_{10}\text{-H}$ solid solution with hydrogen content $n_{\gamma_1}^{\max}$ should behave similarly due to the smallness of the latter value. In particular, since $n_{\gamma_1}^{\max} \rightarrow 0$ at $T \rightarrow 0$ K, $395 \text{ K} \approx T_C(P_{\text{H}_2} = 9 \text{ kbar}) < T_C < T_C(P = 1 \text{ kbar}) = 506 \text{ K}$ in such a sample (see Fig. 2). Hence, samples with $n \geq 0.8$ for which $\sigma_0 = 0$ (Fig. 4a) consist of the γ_2 -phase only. At $0.8 \leq n \leq 1.11$ the paramagnetic susceptibility of the $\text{Ni}_{90}\text{Mn}_{10}\text{-H}$ solutions weakly depends on hydrogen content. The $\sigma^{1.11}(H)$ dependences of the sample with $n = 1.11$ at $T = 4.2$ and 73 K are shown in Fig. 5 (curves 2 and 3). It is seen that as temperature increases, the paramagnetic susceptibility of this sample decreases, and in the chosen scale of axes the $\sigma^{1.11}(H)$ dependence approaches a linear one (in this section the subscripts and superscripts of σ show the temperature and hydrogen concentration, respectively).

For the sample with $n = 0.66$, $\sigma_0 \neq 0$ (Fig. 4a), the magnetization at 4.2 K is strongly dependent on the magnetic field (Fig. 5, curve 4). When temperature increases up to $\approx 70 \text{ K}$, this "paraprocess" noticeably decreases, and the further increase of T (to 130 K) does scarcely change neither the spontaneous magnetization nor the $\sigma(H)$ dependence. Taking into account that under conditions of the experiment $n_{\gamma_2}^{\min} > 0.5 \gg n_{\gamma_1}^{\max}$ and that $\sigma_0 = 0$ at $n \geq 0.8$, one should expect the phase of the $n_{\gamma_2}^{\min}$ composition to have $T_C \ll 298 \text{ K}$. So, the sample with $n = 0.66$ is two-phase. Independent of temperature at $T > 70 \text{ K}$ spontaneous magnetization of this sample is caused by the presence of the γ_1 -phase (of $n_{\gamma_1}^{\max}$ composition), the magnetization dependence on the magnetic field at the same temperatures being a consequence of the large paramagnetic susceptibility of the γ_2 -phase (of $n_{\gamma_2}^{\min}$ composition). In order to determine whether the γ_2 -phase become ferromagnetic below 70 K let us estimate the magnetization $\sigma_{\gamma_2}(H)$ of the part of the specimen with $n = 0.66$ which is in the γ_2 -state. At $T = 100 \text{ K}$ (Fig. 5, curve 5), when the γ_2 -phase is known to be paramagnetic, the spontaneous magnetization of the mixture of the γ_1 and γ_2 phases is $\sigma_{100}^{0.66} \approx (\sigma_{100}^{0.66})_{\gamma_1} \approx 0.08 \mu_B/\text{atom}$ (extrapolation of the $\sigma_{100}^{0.66}(H)$ dependence to $H = 0$ is shown by a dotted line). Since the magnetization of the phase of $n_{\gamma_1}^{\max}$ composition at $T \lesssim 100 \text{ K}$ is nearly independent of H and T (see above), $(\sigma^{0.66}(H))_{\gamma_2} \approx \sigma^{0.66}(H) - \sigma_{100}^{0.66}$ (note, that the sample with $n = 0.66$ contains only $\sigma_{100}^{0.66}/\sigma_0^0 \approx 0.08/0.8 = 1/10$ of the γ_1 phase). The $(\sigma_{4.2}^{0.66}(H))_{\gamma_2}$ dependence is shown in Fig. 5 with a dash-dotted line (curve 6). Extrapolation of this dependence to $H = 0$ using equations [21] yields $(\sigma_{4.2})_{\gamma_2} = 0$. Thus, at atmospheric pressure the γ_2 -phase of the $\text{Ni}_{90}\text{Mn}_{10}\text{-H}$ solution (as well as the γ_2 -phase of the Ni-H solution [22]) is paramagnetic at $T \geq 4.2 \text{ K}$ up to the boundary composition $n_{\gamma_2}^{\min}$.

The spontaneous magnetization of the equilibrium two-phase mixture is a linear function of its composition. As it is seen from Fig. 4a, these demands are well fulfilled for the $\text{Ni}_{90}\text{Mn}_{10}\text{-H}$ system. So, the hydrogen mobility in this system is large enough for the composition of the $(\gamma_1 + \gamma_2)$ -phase mixture to approach near-equilibrium state even at $T \lesssim 150 \text{ K}$ (see above). An approximation of the experimental dependence $\sigma_0(n)$ for the $\text{Ni}_{90}\text{Mn}_{10}\text{-H}$ solutions with $n \leq 0.66$ by a straight line (dashed line in Fig. 4a) yields the value of $\approx 0.7 \approx n_{\gamma_2}^{\min}$ for a hydrogen content at which $\sigma_0 = 0$ (due to smallness of $n_{\gamma_1}^{\max}$, we ignored the change of σ_0 in the region of homogeneity of the γ_1 -phase which does not necessarily follow the dependence shown by a dashed line). Thus, alloying of nickel with manganese up to 10 at % Mn changes weakly both T_{cr} (Section 3.1) and $n_{\gamma_2}^{\min}$.

3.2.2 The $Ni_{80}Mn_{20}$ -H solutions

As mentioned above (Section 3.1), at $x_{Mn} > 0.1$ the critical temperature in the Ni–Mn–H system rapidly decreases and at $x_{Mn} \approx 0.18$ reaches room temperature. No separation into the γ_1 and γ_2 phases is observed for the samples with $x_{Mn} = 0.193$ at atmospheric pressure even at 77 K [18]. Thus, in the range of temperatures and pressures used in the present work, hydrogen must form a continuous series of solid solutions with $Ni_{80}Mn_{20}$ and $Ni_{70}Mn_{30}$ alloys.

The behaviour of the Curie points of the alloy with 20 at% Mn under high hydrogen pressure is shown in Fig. 3. In contrast to the alloy with 10 at% Mn (Fig. 2), hydrogenation at this alloy may result in irreversible changes of T_C . The starting $Ni_{80}Mn_{20}$ alloy has $T_C = (353 \pm 3)$ K. Rapid heating at $P_{H_2} = 0.8$ kbar up to 420 K with exposure at this temperature for 30 min to saturate the sample with hydrogen up to the equilibrium value resulted in an increase of its Curie point up to ≈ 370 K (triangles in Fig. 3). A similar procedure at $P_{H_2} = 4.8$ kbar resulted in an increase of T_C up to ≈ 420 K (circles in Fig. 3), the anomaly of the $\mu_0(T)$ dependence corresponding to T_C , becoming greatly stretched in temperature. On further step-wise increase of pressure with steps of ≈ 1 kbar, the Curie points steadily decreased in both cases. On lowering the pressure, the Curie points fell approximately to the same curves as for pressure increase and did not return to the T_C values of the starting alloy. Such a phenomena had not been observed before on studying hydrogen solutions in Ni [17], Ni–Fe [16, 24], Ni–Co [25, 3], and Ni–Mn alloys with 10 at% Mn (see Fig. 2).

The Curie points of the Ni–Mn alloys may undergo a drastic change at plastic deformation of the samples. For instance, rolling of the sample with 20 at% Mn at room temperature from a thickness of 0.2 to 0.08 mm resulted in a decrease of T_C from 353 to 317 K. The detected increase of T_C on the initial rapid saturation of this alloy with hydrogen is apparently associated with just the crystalline structure defects formed during this process (introduction of $n = 0.7$ of hydrogen into the Ni–Mn alloys produces an $\approx 18\%$ increase of their volume [18]). An increase of the Curie points of our alloys might have been caused by their ordering [12]. However, this possibility should be excluded, since after the exposure of the specimens which were used to obtain the data shown in Fig. 3, to room temperature and atmospheric pressure for several weeks their Curie points returned to the initial value of $T_C \approx 353$ K, the latter would have been impossible in the case of ordering (no additional hydrogen was given off from the specimens). It should be noted that the possibility of irreversible changes of magnetic properties of transition metal alloys on hydrogenation shown in this work makes one to treat with care the results of the experiments with Me–H samples obtained using electrochemical techniques, i.e. under the conditions which are known to be non-equilibrium and hardly controllable ones.

So, if we discard the effects associated with the irreversible changes of T_C , the increase of hydrogen concentration, as is seen from Fig. 3, results in lowering of the Curie points of the $Ni_{80}Mn_{20}$ -H solutions to room temperature already at $P_{H_2} \lesssim \lesssim 10$ kbar. The sample saturated with hydrogen to $n = 0.91$ at $p_{H_2} = 70$ kbar and $T = 520$ K had $T_C \approx 100$ K at atmospheric pressure. Thus, the Curie points of the $Ni_{80}Mn_{20}$ -H solution steadily decrease with hydrogenation.

The irreversible changes of T_C observed for the alloy with 20 at% Mn are not accompanied, however, by such changes of σ_0 exceeding the measurement error. It is seen from Fig. 4a that on hydrogenation of this alloy σ_0 increases, reaches its maximum value of $\approx 0.82 \mu_B/\text{atom}$ at $n \approx 0.37$, and begins to decrease. A similar change of σ_0 for the $Ni_{80}Mn_{20}$ alloy also occurs on substitution of nickel by manganese: σ_0 increases to $\approx 0.8 \mu_B/\text{atom}$ at $x_{Mn} = 0.1$, subsequently decreasing to $\sigma_0^{Ni} = 0.606 \mu_B/\text{atom}$ [20].

Thus, similar to the previous observations for hydrogen solutions in the Ni-Fe [1], $\text{Fe}_{65}(\text{Ni}_{1-x}\text{Mn})_{35}$ [2], and Ni-Co [3] alloys, an increase of hydrogen concentration in the $\text{Ni}_{80}\text{Mn}_{20}$ alloy results in the same change of σ_0 as the increase of the content of an element with a greater number of 3d + 4s electrons. Following [1 to 3], we introduce the coefficients $\xi = -\Delta x_{\text{Mn}}/\Delta n$ and $\zeta = \Delta N^e/\Delta n$ connecting the changes of composition and, respectively, N^e concentrations of the 3d + 4s electrons per atom of the starting alloy, with the changes of n resulting in the same changes of σ_0 (in the case of the Ni-Mn alloys $\zeta = 3\xi$). Then for the position of the maximum of the $\sigma_0(n)$ dependence for the $\text{Ni}_{80}\text{Mn}_{20}$ -H solution (\square in Fig. 4a) we have $\xi \approx 0.1/0.37 \approx 0.27$; $\zeta = 0.81$. Assuming that ξ does not depend on n , we obtain $n = 0.2/\xi \approx 0.74$ for the composition of the solution for which $\sigma_0 = \sigma_0^{\text{Ni}}$. The obtained point is marked with a cross in Fig. 4a and agrees with the experimental dependence $\sigma_0(n)$ for the alloy studied.

It may be relevant to note here that the monotonous decrease of the spontaneous magnetization on hydrogenation of the $\text{Ni}_{80.7}\text{Mn}_{19.3}$ alloy at temperatures close to room temperature [10, 11] does not contradict the $\sigma_0(n)$ dependence for the $\text{Ni}_{80}\text{Mn}_{20}$ alloy found in the present work (Fig. 4a). In fact, according to our data an increase of hydrogen content in the $\text{Ni}_{80}\text{Mn}_{20}$ -H solution should lead to a decrease of the Curie point and, consequently, to a reduction of the spontaneous magnetization at room temperature due to an increase of the relative temperature T/T_C of the measurement. As is seen from Fig. 2 and 3, T_C of this solution should drop below 300 K at $P_{\text{H}_2} \approx 10$ kbar in good agreement with the data of [11].

3.2.3 $\text{Ni}_{70}\text{Mn}_{30}$ -H solutions

The $\text{Ni}_{70}\text{Mn}_{30}$ alloy is paramagnetic at $T \geq 4.2$ K. As is seen from Fig. 4b, the introduction of hydrogen leads to its ferromagnetic ordering. At $n = 0.9$, σ_0 of the $\text{Ni}_{70}\text{Mn}_{30}$ -solution reaches values close to the maximum ones in the Ni-Mn alloys, the Curie point growing to ≈ 250 K. Similar to the case of the alloy with 20 at% Mn, hydrogenation of the samples with 30 at% Mn results in irreversible changes of their magnetic properties, the effect being strongly dependent both on the conditions of the $\text{Ni}_{70}\text{Mn}_{30}$ -H solution preparation, and on the conditions of their decomposition into metal and molecular hydrogen. For instance, after a complete release of hydrogen, the samples sometimes possessed a spontaneous magnetization $\sigma_0 \ll \sigma_0(n)$ disappearing after exposing them for several days to normal conditions. The occurrence of irreversible changes of σ_0 on hydrogenation allows to consider the data shown in Fig. 4b as only semiquantitative estimates.

Assuming the mean value of σ_0 of the four samples grouped close to $n = 0.85$ in Fig. 4b, to be the σ_0 for the $\text{Ni}_{70}\text{Mn}_{30}$ -H solution of this concentration (\square in Fig. 4b) and taking into account that it is the Ni-Mn alloy with 16.5 at% Mn which has such a value of spontaneous magnetization [20], we obtain $\xi \approx (0.3 - 0.165)/0.85 \approx 0.16$. The $\sigma_0(n)$ values calculated using this value of ξ on the basis of the $\sigma_0(x_{\text{Mn}})$ dependence for the Ni-Mn alloys [20] are marked with crosses in Fig. 4b, and a continuous curve is drawn through them. As is seen from the figure, the experimental σ_0 values do not contradict the calculated $\sigma_0(n)$ dependence. Thus, in this alloy the effect of hydrogen on σ_0 also turns out to be similar to that on the substitution of manganese by nickel. Moreover, in the case of the $\text{Ni}_{70}\text{Mn}_{30}$ alloy, as well as in the case of the Ni-Fe [1], $\text{Fe}_{65}(\text{Ni}_{1-x}\text{Mn}_x)_{35}$ [2], and Ni-Co [3] alloys, such an analogy (if only by the order of magnitude) also takes place for the $T_C(n)$ dependence. In particular, on hydrogenation of the $\text{Ni}_{70}\text{Mn}_{30}$ alloy up to $n = 0.85$ (the σ_0 value for this composition of the solution is marked by \square in Fig. 4b), its Curie point steadily increases up to $T_C \approx 250$ K, and the $\text{Ni}_{83.5}\text{Mn}_{16.5}$ alloy (which has the same value of σ_0) shows a T_C as high as ≈ 400 K [12].

4. Discussion

The experimental data show that the $\sigma_0(n)$ dependences for all the investigated Ni-based Me-H solid γ -solutions except for the Ni-Cr-H [9] are similar to the corresponding $\sigma_0(x_{\text{Ni}})$ dependences for the starting alloys. Such a similarity among the $T_{\text{C}}(n)$ and $T_{\text{C}}(x_{\text{Ni}})$ dependences is violated already for the Ni-Cr alloys as well as for the Ni-Mn alloys with 10 and 20 at% Mn (see Section 3.2). It will be shown below that the band theory allows to give at least a qualitative account for the behaviour of the $\sigma_0(n)$ and $T_{\text{C}}(n)$ dependences for all the investigated Me-H systems considering hydrogen as a donor of a fractional quantity of electrons.

4.1 Strong itinerant ferromagnets

The assumption [2, 3] that the effect of hydrogen on the magnetic properties of γ -alloys of transition metals may be described by considering the increasing degree of occupation of the d-states of the starting metal as the main effect, was based on the fact that in the case of Ni-Fe [1], $\text{Fe}_{65}(\text{Ni}_{1-x}\text{Mn})_{35}$ [2], and Ni-Co [3] alloys this effect is similar to that on enriching the starting alloys with the element having a greater number of 3d + 4s electrons. This, in its turn, suggests that the magnetic properties of the studied alloys (without hydrogen) in sufficiently wide ranges of composition are mainly determined by their electron concentration, N^e .

The latter assumption is to be true in the case of the Ni-Co alloys and Ni-Fe alloys containing ≈ 60 at% Fe. In fact, near $T = 0$ K nickel can be considered as a strong itinerant ferromagnet [26], one half of its d-band (d \uparrow with spins up) being completely filled and the other (d \downarrow with spins down) only partially. On alloying nickel with cobalt or iron, σ_0 approximately linearly increases with concentration, in agreement with the Pauling-Slater curve, and has a slope $\partial\sigma_0/\partial N^e \approx -1 \mu_{\text{B}}/\text{electron}$ [27]. This is precisely the behaviour which should be expected if alloying does not result in a change of the band structure of the metal, only decreasing the degree of occupation of its d \downarrow -subband (i.e. the rigid band model for strong itinerant ferromagnets is valid). Note that in the rigid band approximation hydrogenation of these alloys would lead to $\partial\sigma_0^{\text{r}}/\partial n = -1 \mu_{\text{B}}/\text{atom}$. The experimental values of $\partial\sigma_0/\partial n$ deviate noticeably from $\partial\sigma_0^{\text{r}}/\partial n$ and amount to -0.6 to $-0.4 \mu_{\text{B}}/\text{atom}$ for the Ni-Fe alloys containing 10 to 60 at% Fe [1], -0.76 and $-0.71 \mu_{\text{B}}/\text{atom}$ for the Ni-Co alloys with 30 and 60 at% Co [3]. Thus, hydrogen essentially distorts the metal band structure. According to the band structure calculations [5 to 8], an increase of the number of protons in interstitial sites of transition metals lowers the energy of the states of sp-symmetry resulting in an increase of the number of states below the Fermi energy and, therefore, only a part of electrons (0.4 to 0.1 electron/proton for Pd and Ni [5]), supplied by hydrogen atoms into the conduction band, populates the states above the Fermi energy, the rest occupying the mentioned additional states below it. For strong itinerant ferromagnets this yields $0 > \partial\sigma_0/\partial n > -1 \mu_{\text{B}}/\text{atom}$, $1 > \zeta > 0$ in agreement with the slopes of the experimental dependences $\sigma_0(n)$ and $T_{\text{C}}(n)$ [1, 3].

4.2 Weak itinerant ferromagnets

The $\sigma_0(N^e)$ dependence for the Ni-Fe alloys with $x_{\text{Fe}} \approx 0.62$ [1] $\text{Fe}_{65}(\text{Ni}_{1-x}\text{Mn})_{35}$ [2], and Ni-Mn alloys with $x_{\text{Mn}} \approx 0.1$ deviates from the Pauling-Slater curve towards lower σ_0 values [27], the effect being associated probably with the appearance of holes in the d \uparrow -subband (e.g. according to [28], holes in both d-subbands of the Ni-Fe alloys appear at $x_{\text{Fe}} \approx 0.63$). In this case the role of the electron concentration in changing the magnetic properties appears to be more problematic than in the case of alloys in which holes exist only in one d \downarrow -subband. The situation is rather reverse,

the similarity of the behaviour of σ_0 (and, in most cases, of T_C) on hydrogenation and on increase of the nickel content, detected for the in Ni-Fe [1], $\text{Fe}_{65}(\text{Ni}_{1-x}\text{Mn}_x)_{35}$ [2], and Ni-Mn alloys indicates that in wide ranges of composition ($\Delta N^e \cong \zeta n_{\text{max}} \cong 0.5$) the degree of occupation of the d-band, rather than its deformation, mainly determines the magnetic properties of the starting alloys (without hydrogen). In fact, if the deviations of the $\sigma_0(N^e)$ dependence from the Pauling-Slater one (with the slope $\partial\sigma_0/\partial N^e \approx -1 \mu_B/\text{electron}$) were due to different changes of the band structure in the above alloys, then in each case the effect of hydrogen would be different in principle (in the Ni-Fe alloys it should be opposite to the effect of Fe, in Ni-Mn and $\text{Fe}_{65}(\text{Ni}_{1-x}\text{Mn}_x)_{35}$ opposite to that of Mn), which is unlikely.

Note, however, that the coefficients ζ may be quite phenomenological and do not give any estimate of the fraction of electrons supplied by hydrogen atoms above the existing Fermi level, since these coefficients describe the total effect of hydrogenation upon the magnetic properties including, in particular, that due to an increase of the alloy volume (approaching $\approx 18\%$ at $n = 0.7$ [15, 18, 1 to 3]). For instance, the $T_C(V)$ dependence seems to play a dominant role in T_C varying under hydrogenation of the Ni-Fe alloys containing more than 10 at% Fe [1, 24]. The situation with account of the $\sigma_0(V)$ dependence is more involved. In fact, the maximum values σ_0 achieved on hydrogenation approximately equal those for the starting alloys without hydrogen for Ni-Mn-H and Ni-Fe-H systems (that is, $\sigma_0^{\text{max}} \approx 0.8 \mu_B/\text{atom}$ for $\text{Ni}_{90}\text{Mn}_{10}$ alloy and hydrogenated $\text{Ni}_{80}\text{Mn}_{20}$ alloy, see Section 3.2.2., $\approx 1.8 \mu_B/\text{atom}$ for $\text{Ni}_{38}\text{Fe}_{68}$ alloy and hydrogenated alloys containing 66.1 and 67.5 at% Fe [1]). This is a rather unexpected result, particularly in the case of the Ni-Fe alloys due to the strong dependence of their σ_0 values upon pressure (and, therefore, upon volume). For instance, under the assumption that the $\sigma_0(V)$ dependence is the same on expansion as on compression, the volume expansion on hydrogenation leads to $\partial\sigma_0^V/\partial n|_{n=0} \approx 3.4 \mu_B/\text{atom}$ for the $\text{Ni}_{33.9}\text{Fe}_{66.1}$ alloy [2] having the σ_0 value close to the maximum one, whereas the experiment yields for such a sample $\partial\sigma_0/\partial n \approx 0$ up to $n \approx 0.5$ [1]. Thus, the $\sigma_0(n)$ dependence for the Ni-Fe alloys behaves so as if at normal pressure these alloys have the maximum values of σ_0 possible at a given electron concentration. Unfortunately, any acceptable theory accounting for the behaviour of the magnetic properties of invars is absent at present, and any further discussion in this field is still premature.

Another question to be considered in this section concerns the $\sigma_0(n)$ dependence for the $\text{Ni}_{90}\text{Mn}_{10}$ alloy. Since the γ_2 phase of the $\text{Ni}_{90}\text{Mn}_{10}$ -H solution is paramagnetic at $n \cong 0.7$ (Section 3.2.1), and $\sigma_0^0 = 0.8 \mu_B/\text{atom}$ at $n = 0$ (Fig. 4a), $(\partial\sigma_0/\partial n)_{\text{average}} \cong \cong -\sigma_0^0/n \approx -1.1 \mu_B/\text{atom}$ for this alloy. Such a large value of $|\partial\sigma_0/\partial n|$, however, does not contradict the assumption that hydrogen atoms supply a fractional quantity (less than unity) of electrons above the existing Fermi level, since the $\text{Ni}_{90}\text{Mn}_{10}$ alloy itself is not a strong itinerant ferromagnet (in particular, its σ_0 value lies below the Pauling-Slater curve [27]). In a weak itinerant ferromagnet large values of $|\partial\sigma_0/\partial n|$ are possible due to the appearance of holes in the $d\uparrow$ -subband in addition to the filling of the $d\downarrow$ -subband.

4.3 Ni-Cr-like alloys

Alloying of nickel with chromium and 3d-elements left of it in the Periodic Table sharply decreases σ_0 . Since the decrease of N^e occurring in this case should result in the opposite effect if the rigid band model is valid, the changes of the band structure are to determine the behaviour of σ_0 of these alloys to a considerable degree.

According to Friedel [4] a perturbation potential introduced into nickel by an impurity with nuclear charge $Z \leq Z_{\text{Cr}}$ is repulsive enough to subtract a bound state from the $d\uparrow$ -subband and to shift it above the Fermi energy. Such a virtual state will

empty itself into the conduction band, mainly in the other half of the d-band (with spins down) because of its high density of states, which results in a decrease of σ_0 of the alloy. Consequently, the electrons supplied by the dissolving hydrogen will mainly fill the $d\downarrow$ -subband, too, lowering the magnetization and decreasing the Curie points. This is the behaviour of $\sigma_0(n)$ and $T_C(n)$ which was observed for the Ni-Cr-H solid solutions containing 7 at% Cr in the very good work [9].

As to the Ni-Mn alloys, summarizing the above facts, one can conclude them to exhibit an intermediate kind of behaviour, their $T_C(x_{Mn})$ and $\sigma_0(x_{Mn})$ dependence being determined by the increase of electron concentration, as well as by the changes of the band structure. Note that the role of electron concentration seems to increase as x_{Mn} increases. For instance, both T_C and σ_0 grow on hydrogenation of the Ni₇₀Mn₃₀ alloy in agreement with their dependence for the starting Ni-Mn alloys (Section 3.2.3).

So, hydrogenation should result in a decrease of σ_0 and T_C of the alloys of nickel and 3d-metals with $Z \leq Z_{Cr}$. The same effect should be observed, e.g. on hydrogenation of f.c.c. cobalt alloys with metals with $Z \leq Z_{Mn}$, as the $\sigma_0(N^e)$ dependences for these alloys also have a positive slope. Due to the large density of states at the Fermi level of nickel and cobalt, the electrons supplied by hydrogen will also fill the $d\downarrow$ -subband in f.c.c. alloys of these metals with non-transition elements, again decreasing σ_0 and T_C .

5. Conclusion

The behaviour of σ_0 and T_C of hydrogen solid solutions in f.c.c. alloys of 3d-metals based on nickel shows that their d-bands considerably weaker deforms on hydrogenation than the sp-bands, the degree of occupation of the d-bands growing as n increases. The $\sigma_0(n)$ dependences may be qualitatively described by considering hydrogen as a donor of a fractional quantity of electrons. Such an approach makes it possible to predict the behaviour of magnetic properties of a number of Me-H solutions. For instance, as n grows a decrease of σ_0 and T_C should occur for strong itinerant ferromagnets (Ni-Zn, Co-Fe, see Sections 4.1, 4.2; for the Ni-Cu alloys the disappearance of ferromagnetism on hydrogenation was shown in [30, 31]), for alloys with $\partial\sigma_0/\partial N^e > 0$ at a low impurity content (Ni-V, Ni-Ti, Co-Mn, Co-Cr, etc., see Section 4.3), and for alloys with non-transition elements (Ni-Al, Ni-Be, Ni-Sb, etc. see Section 4.3). An increase of σ_0 on hydrogenation should, probably, be observed only for the Ni-Fe and Ni-Mn alloys (as well as for the alloys based on them, in particular, Fe₆₅(Ni_{1-x}Mn_x)₃₅) in the region of compositions where $\partial\sigma_0/\partial N^e > 0$.

Acknowledgements

The authors wish to thank E. G. Ponyatovskii for stating the problem of investigation, constant support of the work and useful discussions, B. K. Ponomarev who supplied the equipment for magnetic measurements, K. A. Peresada, A. I. Amelin, and A. N. Grachev for their assistance in preparing and conducting the experiments, as well as V. G. Glebovskii in whose group the nickel-manganese alloys were melted.

References

- [1] V. E. ANTONOV, I. T. BELASH, V. F. DEGTYAREVA, B. K. PONOMAREV, E. G. PONYATOVSKII, and V. G. THIESSEN, *Fiz. tverd. Tela* **20**, 2681 (1978).
- [2] V. E. ANTONOV, I. T. BELASH, B. K. PONOMAREV, E. G. PONYATOVSKII, and V. G. THIESSEN, *phys. stat. sol. (a)* **52**, 703 (1979).
- [3] V. E. ANTONOV, I. T. BELASH, B. K. PONOMAREV, E. G. PONYATOVSKII, and V. G. THIESSEN, *phys. stat. sol. (a)* **57**, 75 (1980).
- [4] J. FRIEDEL, *Nuovo Cimento Suppl.* **7**, 287 (1958).

- [5] A. C. SWITENDICK, Ber. Bunsenges. phys. Chem. **76**, 536 (1972).
- [6] A. C. SWITENDICK, in: Topics in Appl. Phys., Ed. G. ALEFELD and J. VÖLKL, Vol. 28, Springer-Verlag, 1978 (p. 101).
- [7] N. I. KULIKOV, V. N. BORZUNOV, and A. D. ZVONKOV, phys. stat. sol. (b) **86**, 83 (1978).
- [8] N. I. KULIKOV, phys. stat. sol. (b) **91**, 753 (1979).
- [9] C. J. ZIMMERMANN and H. J. BAUER, Z. Phys. **229**, 154 (1969).
- [10] H. J. SCHENK and H. J. BAUER, Proc. Internat. Meeting Hydrogen in Metals, Vol. 1, Münster (BRD) 1979 (p. 350).
- [11] H. J. SCHENK, H. J. BAUER, and B. BARANOWSKI, phys. stat. sol. (a) **52**, 195 (1979).
- [12] M. HANSEN and K. ANDERKO, Constitution of Binary Alloys, Vol. 2, McGraw-Hill Publ. Co., Inc., New York/Toronto/London 1958.
- [13] L. JACOBS and P. LAWRENCE, Rev. sci. Instrum. **28**, 713 (1958).
- [14] G. T. DUBOVKA and E. G. PONYATOVSKII, Fiz. Metallov i Metallovedenie **33**, 540 (1972).
- [15] B. BARANOWSKI and R. WISNIEWSKI, Bull. Acad. Polon. Sci., Ser. sci. chim. **14**, 273 (1966).
- [16] E. G. PONYATOVSKII, V. E. ANTONOV, and I. T. BELASH, Dokl. Akad. Nauk SSSR **230**, 649 (1976).
- [17] V. E. ANTONOV, I. T. BELASH, and E. G. PONYATOVSKII, Dokl. Akad. Nauk SSSR **233**, 1114 (1977).
- [18] M. KRUKOWSKI and B. BARANOWSKI, J. less-common Metals **49**, 385 (1976).
- [19] V. E. ANTONOV, I. T. BELASH, B. K. PONOMAREV, E. G. PONYATOVSKII, and V. G. THIESSEN, see [10] (p. 277).
- [20] S. V. VONSOVSKII, Magnetizm, Izd. Nauka, Moskva 1971 (p. 670).
- [21] D. M. EDWARDS and E. P. WOHLFARTH, Proc. Roy. Soc. **A303**, 127 (1968).
- [22] V. G. THIESSEN, V. E. ANTONOV, I. T. BELASH, B. K. PONOMAREV, and E. G. PONYATOVSKII, Dokl. Akad. Nauk SSSR **242**, 1390 (1978).
- [23] B. BARANOWSKI, see [6] (p. 157).
- [24] E. G. PONYATOVSKII, V. E. ANTONOV, and I. T. BELASH, Fiz. tverd. Tela **18**, 3661 (1976).
- [25] V. E. ANTONOV, I. T. BELASH, and E. G. PONYATOVSKII, Fiz. Metallov i Metallovedenie **45**, 884 (1978).
- [26] B. K. PONOMAREV and V. G. THIESSEN, Zh. eksper. teor. Fiz. **73**, 332 (1977).
- [27] J. CRANGLE and G. C. HALLAM, Proc. Roy. Soc. **A272**, 119 (1963).
- [28] G. T. DUBOVKA, phys. stat. sol. (a) **24**, 375 (1974).
- [29] S. V. VONSOVSKII, see [20] (p. 528).
- [30] H. J. BAUER, G. BERNINGER, and G. ZIMMERMANN, Z. Naturf. **23a**, 2023 (1968).
- [31] H. J. BAUER, Z. angew. Phys. **26**, 87 (1968).

(Received January 2, 1980)